A measurement/model comparison of ozone photochemical loss in the Antarctic ozone hole using Polar Ozone and Aerosol Measurement observations and the Match technique

Karl Hoppel and Richard Bevilacqua
Naval Research Laboratory, Washington, D. C., USA

Timothy Canty, Ross Salawitch, and Michelle Santee
Jet Propulsion Laboratory, California Institute of Technology, Pasadena, California, USA

Received 1 December 2004; revised 16 May 2005; accepted 21 June 2005; published 12 October 2005.

[1] The Polar Ozone and Aerosol Measurement (POAM III) instrument has provided 6 years (1998 to present) of Antarctic ozone profile measurements, which detail the annual formation of the ozone hole. During the period of ozone hole formation the measurement latitude follows the edge of the polar night and presents a unique challenge for comparing with model simulations. The formation of the ozone hole has been simulated by using a photochemical box model with an ensemble of trajectories, and the results were sampled at the measurement latitude for comparison with the measured ozone. The agreement is generally good but very sensitive to the model dynamics and less sensitive to changes in the model chemistry. In order to better isolate the chemical ozone loss the Match technique was applied to 5 years of data to directly calculate ozone photochemical loss rates. The measured loss rates are specific to the high solar zenith angle conditions of the POAM-Match trajectories and are found to increase slowly from July to early August and then increase rapidly until mid-September. The Match results are sensitive to the choice of meteorological analysis used for the trajectory calculations. The ECMWF trajectories yield the smallest, and perhaps most accurate, peak loss rates that can be reproduced by a photochemical model using standard JPL 2002 kinetics, assuming reactive bromine (BrOx) of 14 pptv based solely on contributions from CH3Br and halons, and without requiring ClOx to exceed the upper limit for available inorganic chlorine of 3.7 ppbv. Larger Match ozone loss rates are found for the late August and early September period if trajectories based on UKMO and NCEP analyses are employed. Such loss rates require higher values for ClO and/or BrO than can be simulated using JPL 2002 chemical kinetics and complete activation of chlorine. In these cases, the agreement between modeled and measured loss rates is significantly improved if the model employs larger ClOOCl cross sections (e.g., Burkholder et al., 1990) and BrOx of 24 ppt which reflects significant contributions from very short-lived bromocarbons to the inorganic bromine budget.

Citation: Hoppel, K., R. Bevilacqua, T. Canty, R. Salawitch, and M. Santee (2005), A measurement/model comparison of ozone photochemical loss in the Antarctic ozone hole using Polar Ozone and Aerosol Measurement observations and the Match technique, *J. Geophys. Res.*, *110*, D19304, doi:10.1029/2004JD005651.

1. Introduction

[2] Polar ozone loss is an important component of global ozone change and has been the subject of intense study for nearly 20 years. The processes responsible for this loss have now been reasonably well elucidated [*World Meteorological Organization* (*WMO*), 2003]. However, there is evidence that deficiencies remain in our ability to correctly model observed ozone loss, which may impact predictions of ozone trends as stratospheric chlorine decreases, and greenhouse gasses increase. For example, several studies have attempted to simulate chemical loss observed in the wintertime Arctic with photochemical/dynamical models [e.g., *Becker et al.*, 1998; *Lefèvre et al.*, 1994; *Goutail et al.*, 1999; *Douglass et al.*, 1997; *Chipperfield et al.*, 1996a, 1996b; *Deniel et al.*, 1998]. The simulations generally underestimate the observed ozone losses in the lower stratosphere. The polar ozone loss calculation is exceedingly complex, and many factors may contribute to the observed model/measurement discrepancies. There may be problems in the gas phase chemistry, in the heterogeneous chemistry that is responsible for activating chlorine, or in the specification of the dynamics.

0148-0227/05/2004JD005651$09.00

[3] Recently, *Rex et al.* [2003] compared Lagrangian ozone loss rates, derived using the Match technique applied to ECC sonde data for the cold Arctic winters of 1992, 1995, 1996, and 2000 with model calculations. For the 1992 winter, they found that in order to reproduce the largest January loss rates, a reactive chlorine, ClOx (ClO + 2 × ClOOCl), abundance of more than twice the total atmospheric chlorine loading was required. The January loss rates in 1995, 1996, and 2000 also required ClOx amounts that were marginally larger than the maximum chlorine loading. In February and early March of 1996, Microwave Limb Sounder (MLS) ClO observations were also available during a period of rapid ozone loss. In this period, *Rex et al.* [2003] found that the modeled loss rates, constrained with ClOx values derived from MLS ClO measurements, agreed well with the measured loss rates. The January measurement/model discrepancy suggests that there may be a problem in our understanding of ozone catalytic loss cycles, apart from any problems in the heterogeneous chemistry or model dynamics. This led to speculation that the problem is related to ozone chemistry occurring at low temperatures and at high solar zenith angles typically found in January [*Rex et al.*, 2003].

[4] The Antarctic ozone hole is a more favorable venue for examining ozone catalytic loss processes than the Arctic because the dynamics are less complicated First, the Antarctic lower stratosphere becomes sufficiently cold to produce nearly complete denitrification and total chlorine activation every year. Second, the chemical isolation of the vortex is stronger than in the Arctic, where transvortex mixing becomes an important issue. Third, although descent still needs to be accounted for in the Antarctic, below 550 K, descent is very slow during the ozone hole formation period [*Bevilacqua et al.*, 1997]. The Antarctic also presents some unique challenges in characterizing the spatial distribution of ozone and ozone loss within the vortex. The nearly pole centered zonal flow in the Antarctic leads to midwinter loss that is confined to the sunlit outer portion of the vortex, with little mixing into the dark inner region [e.g., *Lee et al.*, 2000]. The highly nonuniform loss rates result in large horizontal ozone gradients as the ozone hole develops. Therefore the position of an ozone measurement with respect to the vortex is more important in the Antarctic than in the Arctic.

[5] There have been many Antarctic ozone hole model/measurement comparison studies, starting with early aircraft and ground based observations [e.g., *Anderson et al.*, 1989; *De Zafra et al.*, 1989]. More recent studies have used MLS measurements to both constrain the model chemistry and to compare directly with the modeled ozone [e.g., *Schoeberl et al.*, 1996; *Chipperfield et al.*, 1996b; *MacKenzie et al.*, 1996; *Wu and Dessler*, 2001]. Although there were measurement/model discrepancies, these studies were generally successful in reproducing the general features of the ozone hole including the timing of the loss and the total amount of loss. In the most recent of these studies, *Wu and Dessler* [2001] compared 3 years of MLS data at 465 K with a photochemical loss calculation that used ClOx values derived from MLS ClO measurements. The agreement between the measured and modeled ozone loss was very good, much improved over that obtained in the previous studies. However, all of these studies focused on vortex average ozone loss, which is difficult to interpret because of the large sensitivity of ozone loss to position within the vortex. In addition, the 5 km vertical resolution of the version 4 MLS retrievals used in these studies is somewhat coarse compared to the single potential temperature level used in the model. In addition to the MLS-based studies, *Lee et al.* [2000, 2002] used the SLIMCAT chemical transport model to simulate the ozone hole, and compared the results to Antarctic ozonesonde observations. Although the ozonesonde measurements are sparse, the comparisons show that the SLIMCAT simulations reproduce the overall distribution of ozone loss inside the vortex.

[6] A good quantitative test of our understanding of ozone loss is to compare model loss rates with Lagrangian-based ozone loss rates inferred from measurements with high precision and vertical resolution (compared to the vertical scale of the ozone hole). In this way the complications due to large-scale transport can be eliminated. The ''Match'' technique, originally developed by *Von der Gathen et al.* [1995], applied to high-resolution solar occultation measurements, is one such method for directly estimating ozone loss rates.

[7] The Polar Ozone and Aerosol Measurement (POAM) II and III instruments have provided a unique 9-year record of high–vertical resolution measurements of ozone in the ozone hole region (POAM II: 1994–1996, and POAM III: 1998 to present and still operational). In this paper we analyze the Antarctic ozone loss inferred from the POAM data, and compare it to calculations made with a trajectory-driven photochemical box model adapted from *Salawitch et al.* [1993]. The paper has three specific objectives. First, we update the POAM ozone hole climatology that was previously presented by *Bevilacqua et al.* [1997] using only POAM II data. Second, we use the photochemical box model to produce season-long model simulations of POAM ozone measurements in the ozone hole for several years. Third, we use the Match technique to infer ozone loss rates in the ozone hole from the POAM measurements, and compare these rates to model rates calculated along the Match trajectories.

2. POAM III Ozone Data

[8] The POAM instruments [*Lucke et al.*, 1999] have provided a unique 9-year record of ozone hole measurements (POAM II: 1994–1996; POAM III: 1998 to present). POAM is a solar occultation instrument that typically makes 14–15 measurements per day in each hemisphere around a circle of latitude with a longitudinal spacing of about 25°. The latitudinal measurement coverage as a function of time is identical each year, and is shown for the Southern Hemisphere (SH) in Figure 1 during the ozone hole time period. The lowest latitude (65°S) is sampled at solstice, and highest latitude (88°S) is sampled at equinox. From the beginning of April to the middle of September the POAM measurement latitude follows the edge of the polar night, and from July through September nearly all measurements are made inside the polar vortex [e.g., *Bevilacqua et al.*, 1997].

[9] *Bevilacqua et al.* [1997] have presented a climatology of POAM II measurements of the ozone hole. In this study, we focus on the POAM III (hereafter denoted simply as

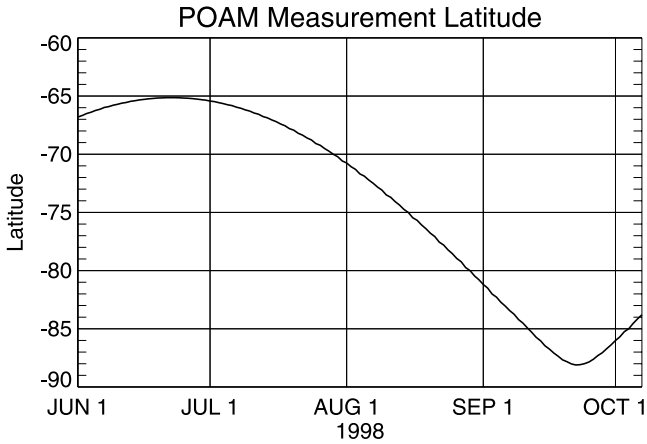

Figure 1. POAM Southern Hemisphere measurement latitude.

POAM) measurements. We use version 3 POAM retrievals (the current operational version), which have been described by *Lumpe et al.* [2002a], and validated by *Lumpe et al.* [2002b], *Randall et al.* [2003], *Prados et al.* [2003], and *Danilin et al.* [2003]. At 15 km and above, the ozone retrievals have a vertical resolution of about 1 km, and an estimated precision of 5% [*Lumpe et al.*, 2002a].

[10] Figure 2 shows the in-vortex ozone mixing ratio time series for all six POAM measurement years during the Antarctic winter/spring season on the 495 K potential temperature surface. Each line represents an 11-day moving average of all POAM measurements inside the vortex, using the vortex delineation algorithm of *Nash et al.* [1996] (middle edge) and the UKMO (United Kingdom Met Office) meteorological analysis. For all years other than 1998, Southern Hemisphere measurements were only made every other day, resulting in 5–6 days of data in the averages shown. Although there is some interannual variation, the character of these time series is remarkably similar from year to year, exhibiting a slow decrease through August, a more rapid decrease beginning in September, and a minimum near zero by October. The one notable exception is 2002, in which an unusual major stratospheric warming occurred in late September [e.g., *Allen et al.*, 2003; *Sinnhuber et al.*, 2003]. An analysis of the 2002 POAM

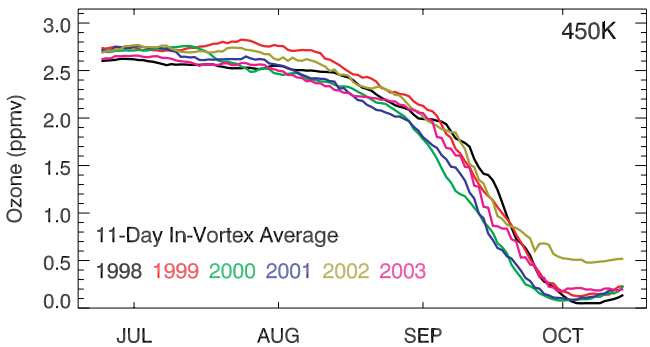

Figure 2. Average ozone time series for all of the POAM III winters. An 11-day moving box average was applied to the measurements inside of the polar vortex.

ozone measurements showed that ozone loss was nominal before the warming, but virtually ceased after the warming, resulting in the much higher minimum ozone mixing ratios at the end of the ozone loss period in early October [*Hoppel et al.*, 2003].

[11] A typical example of the evolution of the ozone profile as sampled by POAM is illustrated in Figure 3, which shows 7-day average in-vortex mixing ratio profiles during the 1998 ozone hole formation. Figures 2 and 3 indicate that most of the ozone decrease at the POAM measurement latitude occurs in September. The region of nearly complete ozone loss extends from 400 to 520 K, and between 520 and 600 K the ozone mixing ratio increases very rapidly with increasing potential temperature.

3. Modeling of the POAM Ozone Hole Observations

[12] As noted earlier, ozone mixing ratios and ozone loss rates can be highly nonuniform within the vortex. Therefore the POAM ozone measurements must be interpreted in the context of the measurement sampling. Since the POAM latitude follows the terminator during the ozone hole period, POAM measurements are made at the boundary between the sunlit outer vortex, in which ozone photochemical loss is occurring, and the dark inner vortex. In addition, ozone reduction rate (slope of the Figure 2 ozone time series) can differ substantially from the local photochemical loss rate occurring at the POAM latitude. This is because POAM does not sample a constant air mass. Therefore even weak meridional transport or mixing in the presence of large latitudinal ozone gradients, obtained in the vortex during the ozone hole formation period, can cause the ozone reduction and local photochemical loss rates to differ. Although the POAM time series is not well suited for specifying the time dependence of the ozone photochemical loss, it is suitable for calculating the cumulative ozone loss over the entire winter, as has been done for 9 years of POAM II and III data

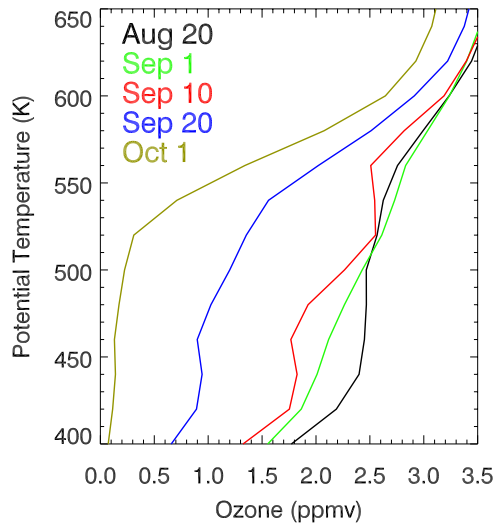

Figure 3. Average ozone profiles at the POAM measurement latitude during the formation of the 1998 ozone hole. Each line is a 7-day average of all measurements inside the polar vortex.

in the analysis of *Hoppel et al.* [2003]. However, since the cumulative loss is nearly complete each year, this is not a very sensitive test of ozone photochemistry.

[13] Because of these limitations, accurate interpretation of the POAM data requires use of a model that accounts for both photochemistry and dynamics. Here we have used a simple trajectory-driven photochemical box model [*Salawitch et al.*, 1993], which has been modified to run along trajectories by *Canty et al.* [2005]. The model calculates ozone loss from chlorine and bromine reactions, while neglecting nitrogen reactions. The chemically active species include O_3, O, ClO, ClOOCl, OClO, HOCl, BrO, BrCl, and HOBr. The amount of total reactive chlorine ClOx (ClO + 2 × ClOOCl) and total reactive bromine, BrOx (BrO + BrCl) are held constant and are specified as inputs to the model. Nitrogen reactions contribute very little (<3%) to ozone loss in the denitrified Antarctic polar vortex [*Lee et al.*, 2002]. The primary impact of nitrogen oxides is on the ClOx level, which is directly specified in the model. Thus the model treats the predominant winter time polar ozone catalytic loss cycles in detail, but does not include the heterogeneous or gas phase chemistry that establishes the ClOx abundance. Unless specified otherwise, JPL 2002 kinetics [*Sander et al.*, 2003] are used. For the baseline model run, the BrOx mixing ratio was set at 20 pptv, which is the total inorganic bromine budget (Br_y) for the time period under consideration, based on contributions from CH_3Br, halons CH_2Br_2 and CH_2BrCl, and other shorter-lived bromocarbons [*Wamsley et al.*, 1998; *Pfeilsticker et al.*, 2000; *WMO*, 2003]. This level of Br_y is an intermediate value between the assumptions used in most global models (i.e., contributions to Br_y only from CH_3Br and halons, leading to Br_y of ~18 pptv and BrOx of ~14 pptv [*Canty et al.*, 2005, Figure 3]) and levels of BrOx inferred from measured BrO in the Arctic vortex, which can be as high as 24 pptv [*Canty et al.*, 2005, Figure 3]). Section 5 explores the effects on ozone loss of increasing BrOx to account for contributions from short-lived organics [e.g., *WMO*, 2003, chapter 2,] and of adopting the ClOOCl cross section of *Burkholder et al.* [1990].

[14] For the POAM III years, there are insufficient Antarctic ClO measurements with which to constrain the model chlorine chemistry. We have therefore run the model using a few selected, illustrative values of ClOx. The stratospheric loading of inorganic chlorine (Cly) reached a peak value of about 3.7 ppbv in the year 1997 [*WMO*, 2003, Figure 1–23]. Although 3.7 is an upper limit to the available reactive chlorine, chemical transport models (CTM) routinely find maximum values of ClOx of ~3.2 ppbv [*Konopka et al.*, 2005; *Lee et al.*, 2000]. Assuming full chlorine activation in the Antarctic throughout the ozone hole period provides an upper limit on ozone loss rates, and is also a reasonable assumption when modeling the evolution of the ozone in the vortex core. *Wu and Dessler* [2001], in an analysis of MLS ClO data, found ClOx values above 3.0 ppbv at equivalent latitudes of 80–85° until just before 20 September. *Shindell and de Zafra* [1997] made ClO profile measurements from McMurdo station (77°S) in 1993 and found that ClO remained activated (peak ClO mixing ratios of 1.8 ppbv) until about 1 October. Furthermore, the modeling analysis given by *Shindell and de Zafra* [1997] suggests that chlorine will remain activated as long as PSCs are present. *Nedoluha et al.* [2003] analyzed POAM II and III PSC measurements and showed that at the POAM measurement locations, PSCs remain present through the end of September each year, with the exception of 2002 (the year with the major warming). *Santee et al.* [2003] have presented a 7 year MLS ClO climatology that shows that the highest ClO values generally persist from the middle of July through the first or second week of September at equivalent latitudes of 75–90°. Lower values of ClO are found near the vortex edge, which is an important feature for the interpretation of ozone loss rates sampled near the edge (see section 5).

[15] In order to simulate the Antarctic ozone hole formation, we ran the box model along an ensemble of trajectories from the end of June to the beginning of October. We began with 3841 parcels at 500 K on 28 June uniformly distributed over the polar region. The initial ozone mixing ratio was assigned from an ozone–potential vorticity relation determined from the POAM measurements over the last 2 weeks of June, in a manner similar to that described by *Randall et al.* [2003]. We use the *Bowman* [1996] diabatic trajectory model driven by UKMO winds to advect these parcels until 1 October. We also performed calculations using the European Centre for Medium-Range Weather Forecasts (ECMWF), and National Centers for Environmental Prediction (NCEP) winds (discussed further in the next section). The ozone mixing ratios evolve in time as determined by the box model run along each parcel trajectory. In order to account for small-scale horizontal mixing, a primitive mixing scheme was employed that simulates a mean horizontal diffusivity of 1.2×10^4 m^2/s, as suggested by *Konopka et al.* [2004, 2005]. The addition of the mixing scheme has a very small effect on the overall ozone distribution, and it has no appreciable impact on the results presented here.

[16] The simulation for 2003 is illustrated in Figure 4. In this case, the parcels were initialized at 500 K and then descended throughout the simulation, reaching an average potential temperature of about 470K by October. The results clearly show that ozone loss begins at the edge of the vortex, then roughly follows the terminator (indicated by the POAM latitude, black circle) toward the pole. It is important to point out that, because our model calculations assumed full chlorine activation throughout the simulation, the ozone loss at the vortex edge and in the edge filaments may be too large. However, the general character of the simulation (ozone loss following the terminator) is in agreement with the SLIMCAT CTM model calculations by *Lee et al.* [2000].

[17] To compare the simulation with the POAM measurements, all the model parcels within ±2° of the POAM latitude have been averaged at each model time step, and the POAM measurements have been interpolated vertically to the average model parcel potential temperature. The results are illustrated in Figure 5 for model ClOx values of 2.8 ppbv and 3.7ppbv. These two ClOx values span the expected range of the average ClOx in an activated vortex.

[18] The most glaring discrepancy between modeled and measured ozone occurs in September 1998, when the model ozone mixing ratio minimizes nearly two weeks earlier than the data. The low values of modeled ozone for September 1998 also occur earlier than either the model or measurements in any other year. The likely cause of this anomalous

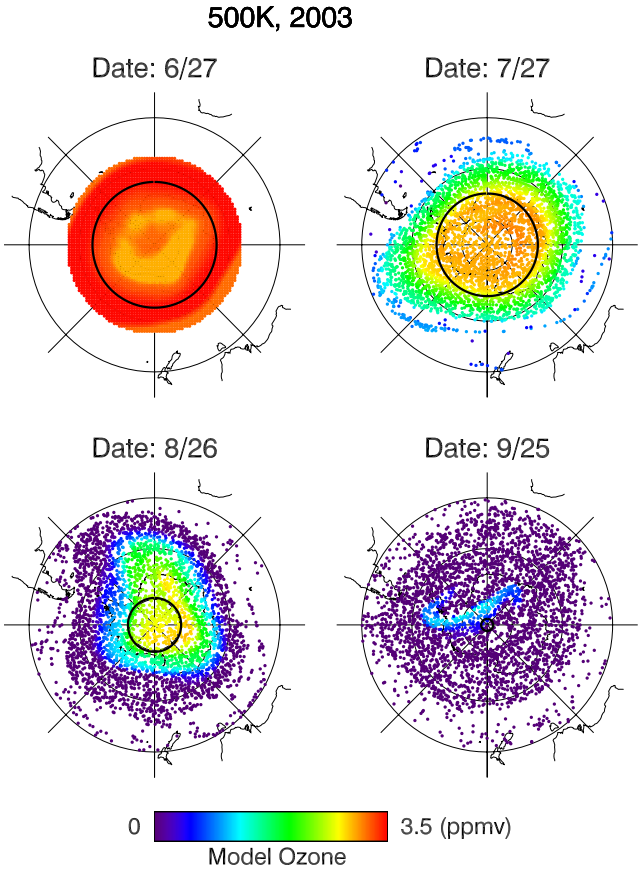

Figure 4. Model ozone distribution for 4 selected dates for the 2003 simulation. Each model air parcel, initialized at 500 K (on 6/27), is shown as a colored circle. The latitude of the POAM measurement is denoted by the black circle.

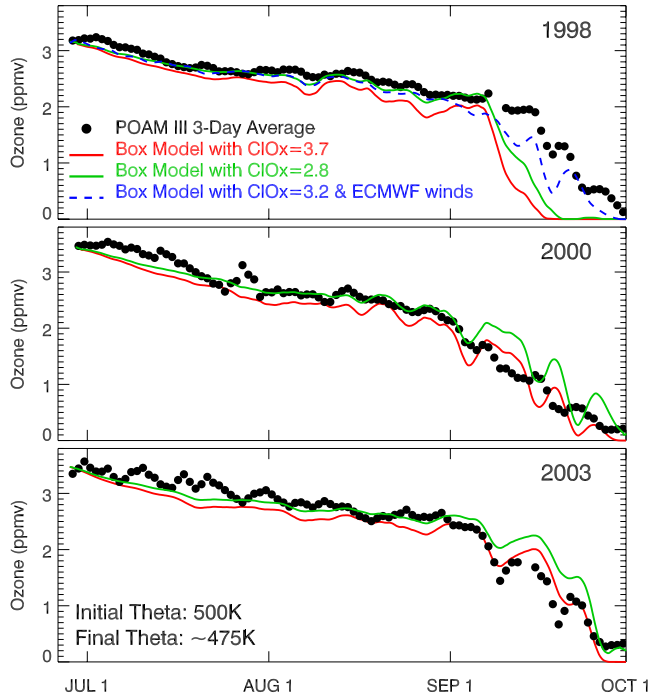

Figure 5. Comparison of the POAM and model ozone time series for 3 years. Only the model air parcels within ±2° of the POAM latitude were averaged. The POAM measurements for each day were sampled at the average potential temperature of the model trajectories, which were initialized at 500 K and descended to about 475 K. UKMO winds were used for all model runs except for the single case in 1998 as indicated.

model result is illustrated in Figure 6. Here we compare the model ozone on 15 September, for 1998 and 2003. The 2003 result is typical, with POAM sampling the highest in-vortex mixing ratios near the pole at this time. However, in the 1998 simulation, the region of relatively high ozone mixing ratio air has drifted off the pole to lower latitudes, and has been replaced at the pole by air that has been in sunlight and is already ozone depleted. There is no suggestion of this in the measurements. In fact, Figures 2 and 5 show that in 1998 the POAM zonal average ozone mixing ratio on 15 September is somewhat higher than found in other years, and the mixing ratio reaches its minimum value a few days later than in other years. Figure 6 suggests, then, that the 1998 measurement/model discrepancy is the result of a problem with the input wind fields and not the chemistry.

[19] The discrepancy for September 1998 illustrates the critical dependence of the measurement/model comparison on the details of the wind field, especially in September when POAM is sampling the small remnant of relatively high ozone. When the 1998 simulation is performed with ECMWF winds (shown also in Figure 5), the agreement is much better because the high ozone remnant remained longer at the POAM latitude. This suggests that errors in the wind fields are the primary reason for the model/measurement discrepancies exhibited in Figure 5. It has been shown that for the Arctic, ozone loss calculations can be very sensitive to the choice of meteorological analysis, due mainly to differences in temperature and hence PSC formation [*Manney et al.*, 2003; *Davies et al.*, 2003]. In the Antarctic vortex, temperatures are usually cold enough that differences between the temperature analyses are less important. Instead, it is the accuracy of the wind analysis

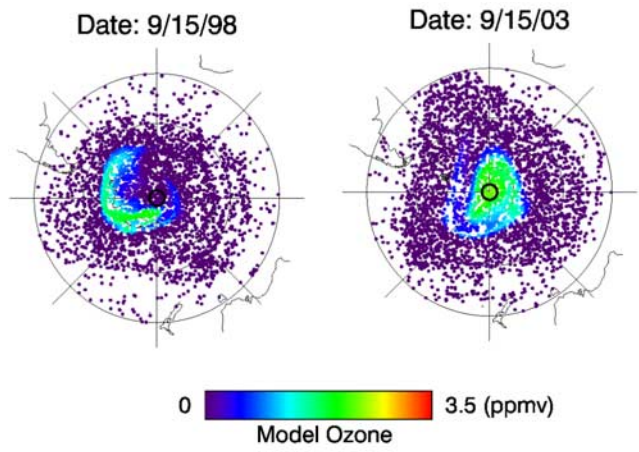

Figure 6. Comparison of the model ozone distribution on 15 September of 1998 and 2003.

inside the vortex that is critical for modeling the POAM measurements.

[20] The measurement/model comparisons shown in Figure 5 for 2000 and 2003 are surprisingly good considering the simple assumption of constant chlorine activation through the winter, for both values of chlorine loading. The total ozone loss is well reproduced, as is the abrupt ozone decrease occurring near 1 September. The agreement may be partly due to the strong isolation of the vortex core [*Lee et al.*, 2001] in which the assumptions of full chlorine activation and denitrification are much better than for the edge (or collar) region of the vortex. Reasonably good model/measurement agreement in the evolution of the ozone hole has been shown before. For example, *Lee et al.* [2000] show good agreement between Antarctic ECC ozonesonde measurements and SLIMCAT model calculations. For a variety of reasons, the approach used here is not adequate to evaluate certain details of photochemical loss of Antarctic ozone. First, the simulation is sensitive to accumulation of errors in the transport fields over the full integration time, as illustrated above. Second, the model/measurement comparison late in the season depends on the cumulative ozone loss throughout the vortex (e.g., regions of the vortex not always sampled by POAM). An examination of ozone along the POAM Match trajectories (described below) isolates the photochemical ozone change, and can be used to test the model representation of changes in ozone loss rate as a function of date and solar illumination conditions. Most importantly, errors do not accumulate in the same manner as for the comparisons shown in Figure 5.

4. POAM Match Analysis

[21] An alternative method of using the POAM measurements to test model photochemistry is to derive Lagrangian loss rates from the data, and compare these rates to model values. In this section, we use this approach by applying the Match technique to the POAM data. Because trajectories used in the application of the Match technique are of relatively short duration (2–10 days) and the model runs used for comparison are initialized with the measured ozone for each trajectory, the errors in the modeled ozone are not cumulative over the entire season.

[22] The Match technique was first developed and applied to ozonesondes by *von der Gathen et al.* [1995], and it has been used to study Arctic ozone loss for many winters [e.g., *Rex et al.*, 1998, 1999, 2002]. The technique has also been applied to satellite occultation measurements by *Sasano et al.* [2000] and *Terao et al.* [2002]. The Match technique used here closely follows these previous analyses. The first step is to use air mass trajectory calculations to locate ozone measurement pairs that sample the same air mass. Ideally, then, the observed ozone change is entirely due to photochemistry. In practice, however, the measured ozone change contains contributions from measurement error and imperfections in the matches (i.e., the sampled air mass is not identical). To reduce the effects of these error sources the ozone loss rates are based on a statistical analysis of many matches rather than a single pair.

[23] The air mass trajectories were calculated using a standard 3-D advection scheme in isentropic coordinates, as described by *Bowman* [1996]. To examine the effect of wind errors on the derived loss rates, the trajectory model was run (and the entire Match analysis performed) independently with horizontal winds obtained from three meteorological analyses. These included the UKMO analysis [*Swinbank and O'Neill*, 1994] (which was used for our baseline calculations), the ECMWF analysis (see http://www.ecmwf.int) (provided by the Norwegian Institute for Air Research (NILU)), and balanced winds derived from the NCEP temperature and geopotential height analysis [*Newman et al.*, 1998]. The time resolution is 12 hours for the UKMO and NCEP data, and 6 hours for the ECMWF data. For the UKMO and NCEP analyses, 3-D trajectories were calculated using the vertical wind (or equivalently the diabatic heating rate in isentropic coordinates) from the radiative transfer model of *Rosenfield et al.* [1994]. This heating rate calculation is not currently available for the ECMWF analysis, so 2-D adiabatic trajectories were used. A vortex average descent calculation was then used to specify a diabatic descent correction for each trajectory. This correction was applied when performing the vertical interpolation of the POAM measurement profile to the trajectory altitude. The descent rates are small for the Match trajectories in this study, so the uncertainties in the heating rate have a minimal effect on the results.

[24] For each POAM measurement location, 10-day forward and backward trajectories were calculated. Each individual trajectory actually consists of a bundle of 7 air parcels arranged as a central parcel and 6 surrounding parcels in a hexagon pattern of radius 110 km. This arrangement encompasses the 200 km by 50 km sampling area of the occultation measurement. A match occurs when, at the time and location of a second POAM measurement, the entire trajectory bundle falls within a specified radius. Requiring the entire trajectory bundle to fall within the Match radius constrains the distance of the central trajectory from the measurement, and also constrains the amount of dispersion or distortion experienced by the bundle. For this work, a Match radius of 1000 km was used. As in the analysis by *Terao et al.* [2002], both the forward trajectory (from first measurement) and the backward trajectory (from second measurement) must meet the above criteria. We experimented with reducing the Match radius, but found no systematic statistical improvement in the final results. This is not surprising since the errors in 5–10 day trajectories likely exceed several hundred kilometers, so that a decrease in the Match radius is not likely to lead to more accurate matches.

[25] The photochemical ozone change that occurs over the 2 to 10 day Match interval is significantly smaller than the random error inherent in the technique. For this reason, we binned the Match pairs into 15-day intervals and calculated 15-day average loss rates. We assume that the ozone change is proportional to the sunlit time along the trajectory, with sunlit time defined as the time duration for which the solar zenith angle (SZA) is less than 92°. This is a simplifying assumption because ozone loss is sensitive to variations in SZA during the sunlit period. However, on the basis of the model results shown here, this is a good approximation for the POAM matches. To illustrate the method, Figure 7 shows the ozone change as a function of the number of sunlit hours for all matched pairs obtained in

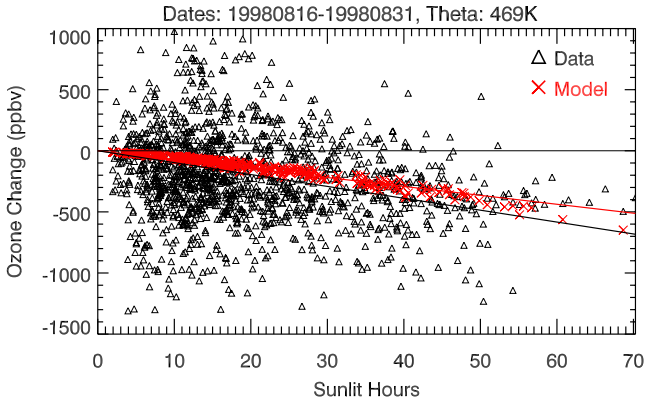

Figure 7. Example plot of the ozone change for each Match pair versus the sunlit time of the Match trajectory for a 15-day time period. The POAM-Match data are shown as black triangles. The black line is a least squares fit constrained to go through zero. The red crosses show the modeled ozone change using the box model along Match trajectories. The red line is the fit to the model data.

the 15-day interval 16–31 August 1998 at 469 K. A linear fit, constrained through zero, is applied to the data to estimate the average loss rate per sunlit time (hereafter referred to as the "Match loss rate"), expressed in units of ppbv per sunlit hour. Figure 7 illustrates the large amount of scatter found in the individual matches. The random measurement error (∼100 ppbv) represents only a small contribution to the scatter. Other error sources include trajectory errors, small-scale mixing, and geophysical variations in true ozone loss rates. All of these error sources are addressed further in this paper. However, here we point out that trajectory errors are likely to be the largest error source because of the large horizontal gradients in the ozone field in the vicinity of the POAM measurements (see Figure 4).

[26] By examining many fits (e.g., Figure 7) it is evident that the scatter often does not follow a Gaussian distribution. If we assume Gaussian error statistics, the calculated standard error of the fit is intuitively too small. *Morris et al.* [2005] have discussed alternative methods for estimating errors in the Match technique. We have chosen an alternative technique that is based on an analysis of the residuals of the linear fits. First, the residual is calculated by subtracting the linear fit from the ozone change data. Next, we assume that the residual (y values) represents random error that is uncorrelated with the sunlit times (x values). Instead of assuming Gaussian statistics for the error, we consider that any rearrangement of the residual x and y values should give an error pattern that is consistent with the data. A linear fit is then applied to many random rearrangements of the x and y values. The RMS combination of the mean and standard deviation of the residual fits is taken as the 1σ error estimate. For the case of true Gaussian error statistics, this alternate σ estimate is about 30% less than the true σ, but for the actual Match fits, the alternate error estimate is always much larger. The error bars shown in the results should be interpreted as ±2σ errors limits.

[27] The ozone loss rate is highly dependent on the SZA, which is an important factor in understanding the POAM-Match loss rates. From the beginning of April to the middle of September, the POAM measurement latitude follows the edge of the polar night. This sampling location, combined with the typically near zonal wind flow, tends to confine the Match trajectories to a region of very high SZA.

[28] Figure 8 shows the frequency distribution of the SZA for the sunlit portion of the POAM Match trajectories for the indicated time periods. Also shown is the SZA distribution (area weighted) for the entire vortex. In early July, the average vortex SZAs and the SZAs sampled by the POAM matches are nearly identical because POAM is sampling near the sunlit vortex edge at this time. From July through mid-September, SZA values for the POAM matches change little and are primarily above 80°. This is expected because the POAM measurements follow the terminator. In contrast, the SZA values for the entire vortex are distributed over a much larger range, and shift toward lower values with time.

[29] Since ozone loss rates increase with decreasing SZA, we expect the POAM-Match loss rates to be smaller than vortex average values. This difference should increase from July to October as the average sunlit SZA in the vortex decreases relative to the Match trajectories. In early October there is a significant shift toward lower SZAs in the POAM matches. In order to account for the peculiar sampling of the POAM matches with respect to SZA, we simulated the ozone loss for the same SZA conditions by running

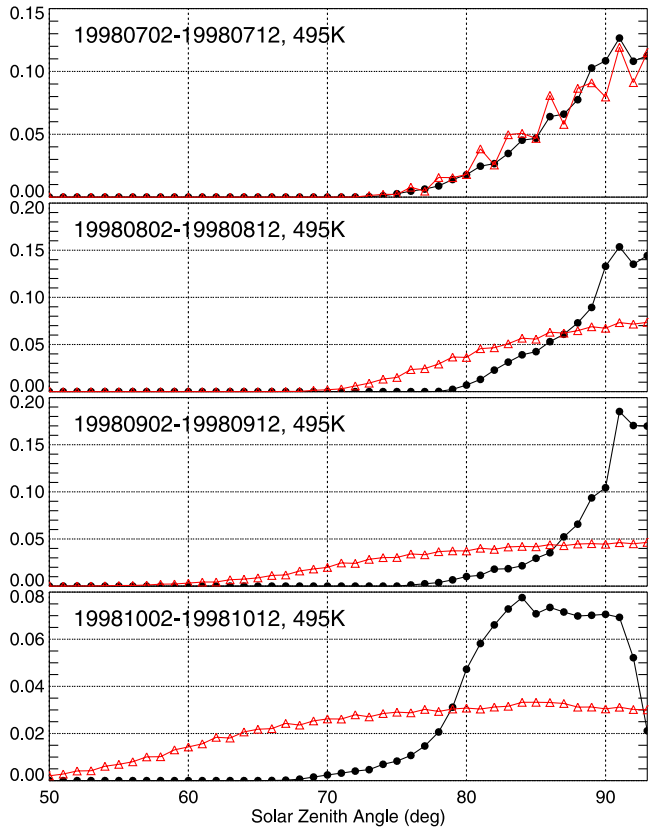

Figure 8. SZA frequency distribution along the Match trajectories (black) and for the entire vortex (red) for the indicated dates at the 495 K level. Only the sunlit portion of the distribution is shown. Matches were identified using UKMO winds.

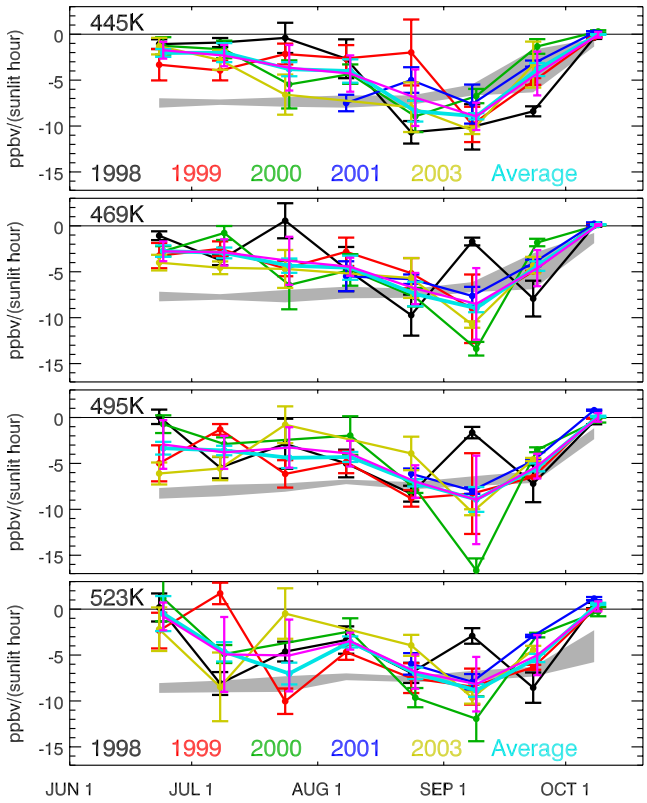

Figure 9. POAM-Match ozone loss rates for 5 years at the indicated potential temperature levels. UKMO winds were used for the trajectory calculations. The calculation of the 5-year average (light blue) is described in the text. The grey shaded region is the range of the photochemical model results for the 5 years, assuming BrOx = 20 pptv and ClOx = 3.7 ppbv.

the model along each POAM match trajectory, initialized with the measured ozone for each match. The modeled ozone changes for the matches were analyzed in the same way as the data, as illustrated in Figure 7. The model results form a compact linear relation and show that the simple linear model is reasonable.

5. Match Analysis Results

[30] The Match loss rates were calculated from mid-June through the end of September (in 15-day increments) for the years 1998, 1999, 2000, 2001 and 2003, using three different meteorological analysis. They were calculated on a fixed potential temperature grid of approximately 0.5 km spacing. In Figures 9–11, we show the results at 4 selected levels, between 445 K and 523 K, which have a spacing of approximately 2 km. In addition to the individual years, we have calculated multiyear average ozone loss by combining the matches for all 5 years for each time bin and potential temperature bin, and performing a single linear fit to determine the ozone loss rate. Combining the years in this way significantly reduces the statistical uncertainty, assuming that the year to year differences in the Match loss rates are dominated by analysis errors rather than by true differences in chlorine and bromine activation. The assumption that the ClOx mixing ratio is similar in each of the 5 years is reasonable because the vortex is stable and cold each year, producing abundant PSCs [e.g., *WMO*, 2003, Figures 3–18 and 3–23]. There is no evidence from the POAM measurements (see Figure 2, excluding 2002) of substantial differences in ozone loss.

[31] The results of these calculations are summarized in Figures 9–11, which show the ozone loss rates based on trajectories calculated using UKMO, NCEP, and ECMWF winds. The Match loss rates exhibit a large degree of year-to-year variability and a large degree of variability between the different wind analyses. However, a general pattern emerges. The Match loss rates generally increase slowly from late June through early August, increase more rapidly later in August reach maximum values in early September, and thereafter decrease. The period of maximum ozone loss occurs in the late August/early September time period.

[32] The year-to-year scatter is largest for the UKMO results, especially for the years 1998 and 2000 in September. Possible wind errors in the 1998 UKMO data have already been noted in section 3. Because of differences in the winds, the set of POAM matches identified using each wind analysis is different. For example, when switching between UKMO and ECMWF winds, we generally find that the number of match pairs that is common to both wind analyses ranges from 20% to 60%, depending on year and potential temperature level. Given that the match sets can differ substantially, it is not surprising that the Match loss rates also differ between wind analyses. Generally, the differences in Match loss rates among the three analyses

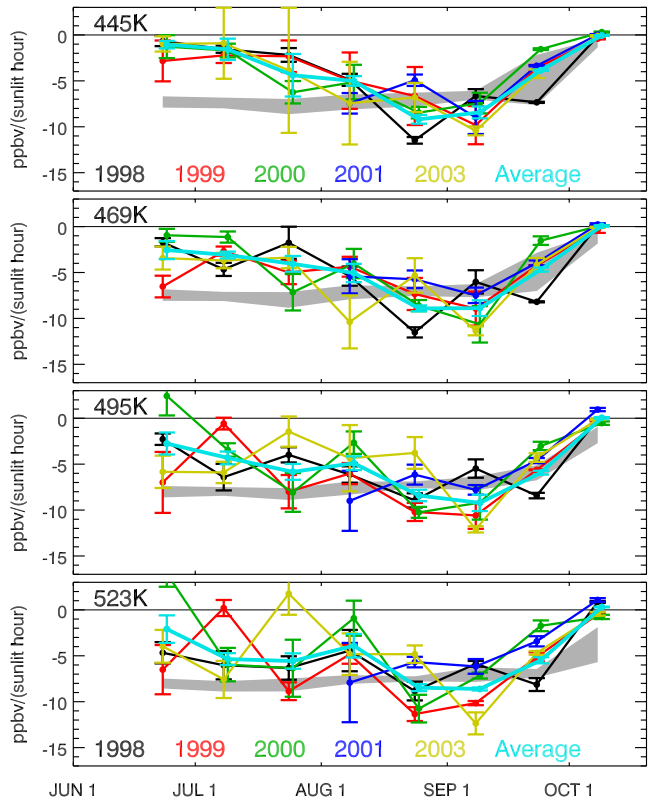

Figure 10. Same as Figure 9 but for the Match results using NCEP winds.

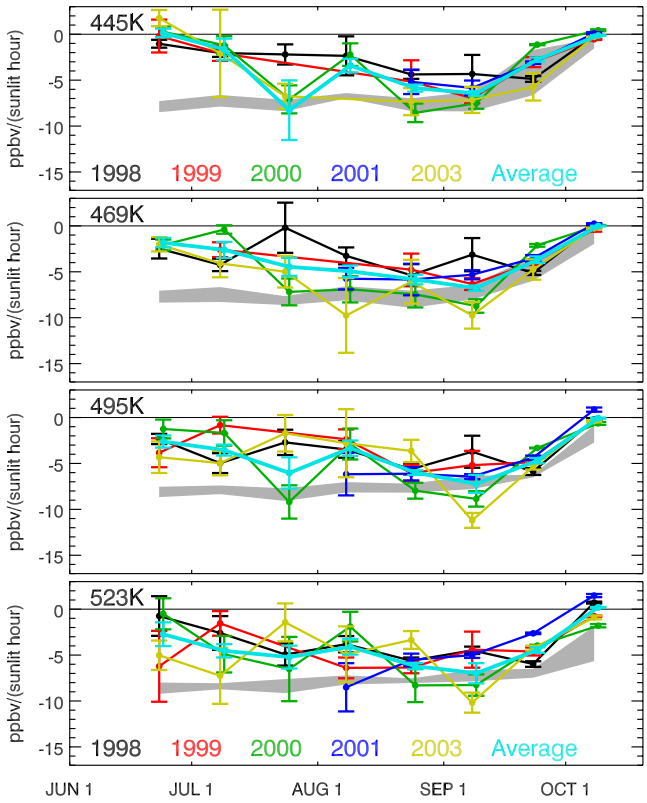

Figure 11. Same as Figure 9 but for the Match results using ECMWF winds.

are in the 1–3 ppbv/sunlit hr range, and are often larger than the statistical error bar calculation. This suggests that a large portion of the year-to-year variability in loss rates may be attributed to trajectory uncertainties. Thus the 5-year average may in fact be a more accurate estimate of ozone loss rates than that of any individual year.

[33] The 5-year average loss rates at 469 K for each wind analysis are shown together in Figure 12. The differences between these 3 time series, most apparent in late August and early September, indicate that the uncertainty due to wind errors is larger than the statistical uncertainty calculated from the fitting of the match data (error bars). The peak ozone loss rates for the 5-year average, which occur in late August and early September, are smallest for the ECMWF analysis. This is true at all 4 potential temperature levels. Assuming other factors being equal, we would expect the ECMWF trajectories to be more accurate because the spatial and temporal resolution of the wind fields is greater [*Rolph and Draxler*, 1990]. For the ECMWF data used here, the spatial resolution is about twice that of UKMO and NCEP, and the temporal sampling is 6 hours compared to 24 hours.

6. Comparisons With a Photochemical Model

[34] As described above, we have also calculated photochemical loss rates, using the box model, along the Match trajectories. These are shown as the gray shaded region in Figures 9–11. These calculations were performed using the same model chemistry as used in the ozone time series simulations presented in Figure 4 and 5 and described in section 3 (i.e., JPL 2002 kinetics, BrOx = 20 pptv, and ClOx = 3.7 ppbv). This baseline chemistry simulates maximum chlorine activation throughout the simulation time period. Thus, assuming the chemical kinetics and BrOx abundance are correct, the results should represent an upper limit to the ozone loss rates.

[35] The model results are similar each year, and nearly constant through mid-September (maximum difference of <1 ppbv/sunlit hour). This is a result of the constant ClOx and BrOx in the model, and the nearly constant SZA distribution shown in Figure 8. The subsequent decrease in the model loss rate at the end of September is largely due to the fact that there is very little ozone left to destroy (see Figure 2). The decrease is not due to a decrease in ozone loss potential because the model ClOx is held constant and the average SZA decreases at the end of September. From mid-June through mid-August the model loss rates generally exceed the Match loss rates, which is consistent with the true ClOx being less than 3.7 ppbv. However, from late August through early September the measured loss rates for individual years often exceed the model results. This suggests a potential problem in the model chemistry.

[36] In order to explore the model chemistry in more detail, we examine the sensitivity of the modeled loss rate to ClOx, BrOx, and the photolysis cross sections of ClOOCl. In each case, we evaluate the results by comparison to the 5-year average Match loss rates shown in Figure 12.

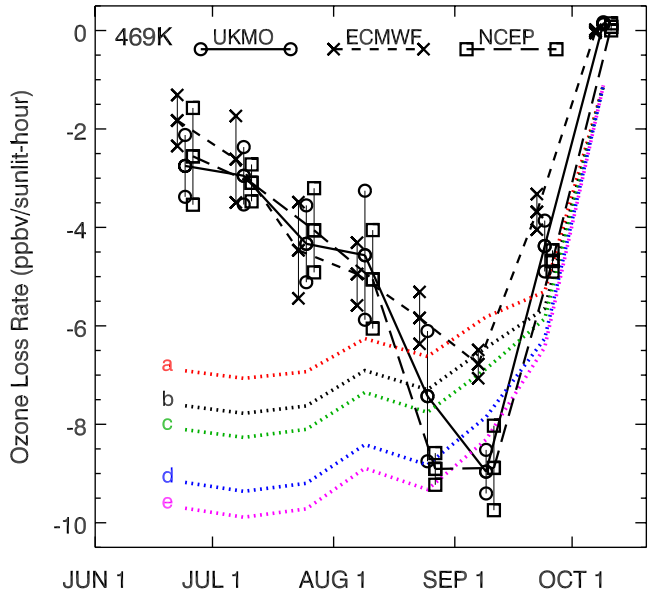

Figure 12. Five-year average Match loss rates using UKMO (circles), NCEP (squares), and ECMWF (crosses) at 469 K. The *x* axis position of the symbols for ECMWF (NCEP) lines have been shifted – (+) 2 days to make the plot easier to read. Model results are shown as dotted lines. The black dotted line is the baseline case (BrOx = 20 pptv, JPL 2002 kinetics). Changes to the baseline are as follows. The red line is BrOx = 14 pptv, the green line is BrOx = 24.1, the blue line is Burkholder ClOOCl cross sections, and the purple line is Burkholder cross sections and BrOx = 24.1 pptv.

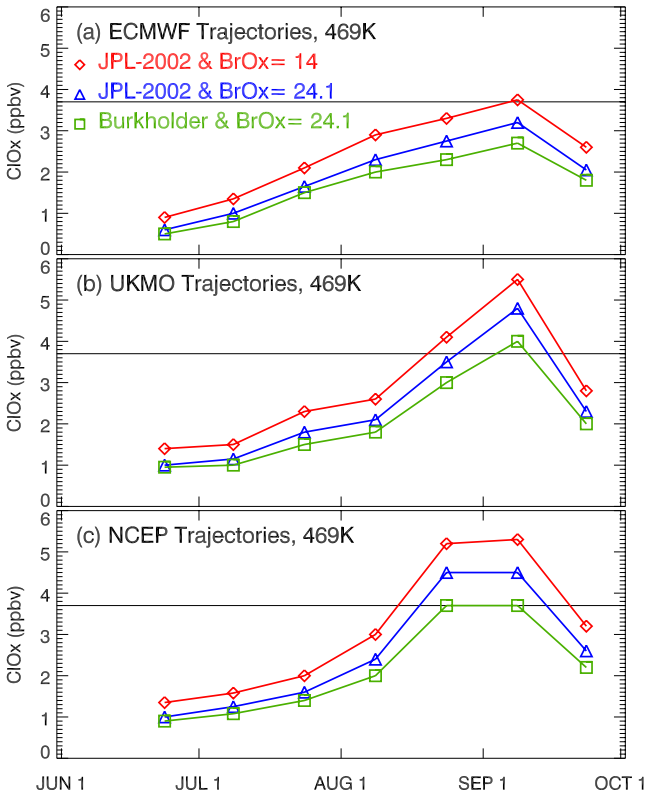

Figure 13. (a) ClOx mixing ratio necessary to reproduce the 5-year average ECMWF Match ozone loss rates for three cases: JPL 2002 ClOOCl cross sections with BrOx = 14 pptv (red diamonds), JPL 2002 cross sections with BrOx = 24.1 pptv (blue triangles), and Burkholder cross sections with BrOx = 24.1 pptv (green squares). (b) Same as Figure 13a but for the Match loss rates based on UKMO trajectories. (c) Same as Figure 13a but using the NCEP trajectories.

[37] First, we consider the sensitivity to BrOx by using upper and lower limit values of 14.0 and 24.11 pptv, used in the analyses of *Canty et al.* [2005]. The smaller value is from the REPROBUS 3D model [*Lefèvre et al.*, 1994] and is based on the assumption of contributions to Br_y from only CH_3Br and halons [*WMO*, 2003]. The larger value was derived from a DOAS balloon-borne measurement of BrO in the Arctic winter [*Fitzenberger,* 2000], and is an upper limit for BrOx in the vortex that would be consistent with a significant contribution to the Br_y budget from short-lived bromocarbons [e.g., *WMO*, 2003, Figure 1–8; *Salawitch et al.*, 2005, and references therein]. Figure 12 shows the model loss rates for the baseline case (black line) and for the upper and lower limiting BrOx values (red and green lines), compared to the average Match loss rates at 469 K. The results show that changing BrOx by nearly a factor of 2 changes the ozone loss rate by about 13%. Using the upper limit BrOx and ClOx values with the JPL 2002 chemistry reproduces the peak Match loss rates calculated using the ECMWF winds, but cannot reproduce the larger loss rates calculated using the UKMO and NCEP winds.

[38] There is significant uncertainty in the ClOOCl cross sections reported in the JPL 2002 recommendation. The cross sections reported by *Burkholder et al.* [1990] are significantly larger longward of 250 nm (by nearly a factor of 10 at 450 nm) than those in the current JPL recommendation. *Stimpfle et al.* [2004], in an analysis of measurements obtained in the SOLVE I campaign, find considerably better agreement in the partitioning of measured ClO and ClOOCl using the Burkholder cross sections than is found using cross sections from JPL 2002 Figure 12 (blue line) shows that for the POAM matches, the ozone loss rates increase by about 18% when the *Burkholder et al.* [1990] cross sections are used. If we combine this change with the larger DOAS derived BrOx values (purple line), the model loss rates are nearly as large as the peak Match loss rates calculated from the UKMO and NCEP winds. This is true for the other potential temperature levels (not shown). Thus we find that using the highest BrOx values consistent with the available data, coupled with the higher Burkholder ClOOCl cross sections and maximum chlorine activation, produces ozone loss rates nearly as large as the largest POAM-Match loss rates.

[39] By setting the BrOx mixing ratio to a constant value, the Match loss rates can be used to infer the time variation of ClOx. Figure 13 shows the ClOx time series that reproduces the Match results for three chemistry cases (JPL 2002 chemistry and BrOx = 14 pptv; JPL 2002 chemistry and BrOx = 24.1 pptv; Burkholder cross sections and BrOx = 24.1 pptv). The Match loss rates suggest that ClOx increases dramatically from the beginning of July to September. The ClOx value required to reproduce the peak ozone loss rate varies by about 1.5 ppbv over the three chemistry cases. For the ECMWF results (Figure 13a), the inferred ClOx ranges from 3.7 ppbv for the standard JPL-2002 chemistry and lowest BrOx (14 pptv) case, down to 2.7 ppbv for the case using the Burkholder ClOOCl cross sections and upper limit BrOx (24.1 pptv). For the UKMO and NCEP results (Figures 13b and 13c)), the inferred ClOx reaches higher than the upper limit Cly (3.7 ppbv) for all three photochemical cases, although for the case of the Burkholder cross sections and upper limit BrOx, the excess ClOx is within the statistical error. Combining the ECMWF loss rates, which are probably the most accurate, with either the upper limit BrOx or Burkholder cross sections results in peak ClOx values that are less than about 3.2 ppbv, a value consistent with many previous modeling studies.

[40] There are no ClOx measurements obtained coincidentally with the POAM measurements with which to compare these results. However, *Santee et al.* [2003] published an Antarctic ClO climatology based on 7 years of MLS measurements. Although the years used for the climatology do not overlap the POAM III years, the meteorology of Antarctic winters is similar for most years. The MLS ClO climatology gives the near noon-time ClO mixing ratio, binned as a function of potential temperature and equivalent latitude. During August and early September the largest value of ClO at 465 K in the climatology is 1.5 ppbv, a value that is nearly constant throughout the vortex core. Using the photochemical model, we have calculated the noon-time ClO corresponding to the inferred ClOx shown in Figure 13, for the latitudes sampled by the match trajectories. For the UKMO and NCEP results, the inferred noon-time ClO in early September exceeds 1.7 ppbv for all 3 of the chemistry cases. For the ECMWF results, the

inferred noon-time ClO does not exceed 1.5 ppbv. This suggests that the large Match loss rates from the UKMO and NCEP trajectories are inconsistent with measured ClO.

[41] We point out that the September time period is particularly challenging for application of the Match technique to POAM measurements. The high rate of ozone decrease observed by POAM at this time is a result of both chemical ozone loss and the transport of low ozone toward the center of the vortex where POAM is sampling. In principal, the Match calculation isolates the chemical loss. In practice, however, trajectory errors can lead to cases where Match pairs do not sample the same air mass. For these cases, we would expect the calculated Match loss rate to be biased toward the average (Eulerian) change observed by POAM, which, in September, is typically larger than the photochemical loss rate. The fact that the UKMO and NCEP based loss rates are larger then ECMWF in September is consistent with the premise that the ECMWF trajectories are more accurate.

7. Summary and Conclusions

[42] The POAM instrument has provided an extensive data set of high–vertical resolution ozone profile measurements in the ozone hole. The measurement latitude follows the edge of the polar night during the ozone hole formation period, and presents a unique challenge for interpreting the observed ozone decrease. We were able to reproduce average time series of the POAM ozone hole measurements (at 450–550 K) using a simple gas phase only, trajectory driven photochemical model. The model includes the primary chlorine and bromine reactions, and assumes full chlorine activation. The success of this model depends on the ability to accurately simulate both horizontal transport and the ozone loss that follows the terminator inward to the pole [*Lee et al.*, 2000]. In early September (for a typical winter), a rapidly decreasing remnant of higher ozone remains near the pole, where POAM is sampling (Figure 6). At this time, model transport errors can have a large effect on the model/measurement comparisons. This was illustrated by the 1998 simulation in which the model ozone decreased to zero about one week ahead of the measured ozone. The time shift was caused by an apparent error in the UKMO winds, which transported the high ozone remnant away from the POAM sampling location.

[43] The season-long model simulations also indicate that there are significant differences between the rate of ozone decrease measured by POAM and the local photochemical loss rate. In order to isolate the photochemical ozone change in the data, the Match technique was applied to 5 years of POAM measurements at four potential temperature levels between 445 K and 523 K. At the POAM measurement latitudes, the measured loss rate per sunlit time generally increased from late June, maximized in early September, and decreased rapidly in late September. By examining the statistical error of the loss rate calculation and the variation arising from the use of different meteorological analyses, we found that trajectory errors (wind errors) account for the largest source of uncertainty.

[44] The photochemical box model was run along the Match trajectories, using a range of ClOx and BrOx values, and using the ClOOCl cross sections of *Burkholder et al.* [1990] in addition to the JPL 2002 recommendation. Using the 5-year average Match loss rates, it was found that for all 4 levels (445 K to 523 K), the large rates, found in early September using the UKMO and NCEP winds, are best simulated in the model using the largest BrOx estimates ($\sim$22–24 pptv), the Burkholder ClOOCl cross sections, and a ClOx abundance of nearly 4.0 ppbv. However, the early September Match loss rates calculated using the ECMWF winds were systematically smaller, and could be reproduced using ClOx levels less than 3.7 ppbv, even for the case of JPL 2002 kinetics and the lowest BrOx estimate. The peak Match loss rates were further evaluated by comparison with the MLS ClO climatology of *Santee et al.* [2003]. The photochemical model was used to convert the ClOx inferred from the Match loss rates to the corresponding noontime ClO for comparison to the climatology. The noon-time ClO corresponding to the UKMO and NCEP Match loss rates exceeded the maximum of the MLS climatology for all chemistry cases, while the ClO inferred from the ECMWF results was within the range of values found in the climatology.

[45] If we consider that the UKMO or NCEP based Match loss rates are correct, then we find that the peak loss rates are larger than model results using JPL 2002 chemistry and reasonable upper limit abundances of ClOx and BrOx. This finding is reminiscent of the conclusion reached by *Rex et al.* [2003] in the ozonesonde-Match analysis of January ozone loss in cold Arctic winters. From July to early September, the POAM-Match loss rates are obtained under conditions of high SZA, low temperatures, and abundant PSCs, similar to that of the Arctic ozonesonde-Match conditions in January.

[46] However, because of the better spatial and temporal resolution, it is likely that the ECMWF trajectories are the most accurate. For the ECMWF based Match loss rates, there is no evidence of a problem in reproducing the measured loss rates. Furthermore, a better quantification of the ClOx at the POAM measurement latitude is necessary to better constrain the model BrOx abundance and choice of ClOOCl cross section.

[47] **Acknowledgments.** Research at NRL was supported in part by the National Aeronautics and Space Administration (NASA) grant ACMAP-0000-0148. Research at the Jet Propulsion Laboratory, California Institute of Technology, is performed under contract with the National Aeronautics and Space Administration. We are grateful to Ken Bowman for providing the original trajectory code and Joan Rosenfield for the heating rate calculations. We thank the European Centre for Medium-Range Weather Forecasts, the Norwegian Institute for Air Research, and the UK Met Office for providing meteorological data. Support for POAM operations and data is provided by NRL, NASA, and the French Centre National d'Etudes Spatiales (CNES).

References

Allen, D. R., et al. (2003), Unusual stratospheric transport and mixing during the 2002 Antarctic winter, *Geophys. Res. Lett.*, *30*(12), 1599, doi:10.1029/2003GL017117.

Anderson, J. G., W. H. Brune, S. A. Lloyd, D. W. Toohey, S. P. Sander, W. L. Starr, M. Loewenstein, and J. R. Podolske (1989), Kinetics of O3, destruction by ClO and BrO within the Antarctic vortex: An analysis based on in situ ER-2 data, *J. Geophys. Res.*, *94*(D9), 11,480–11,520.

Becker, G., R. Muller, D. S. McKenna, M. Rex, and K. S. Carslaw (1998), Ozone loss rates in the Arctic stratosphere in the winter 1991/92: Model calculations compared with Match results, *Geophys. Res. Lett.*, *25*(23), 4325–4328.

Bevilacqua, R. M., et al. (1997), POAM II observations in the Antarctic ozone hole in 1994, 1995, and 1996, *J. Geophys. Res.*, *102*(D19), 23,643–23,658.

Bowman, K. P. (1996), Rossby wave phase speeds and mixing barriers in the stratosphere. part I: Observations, *J. Atmos. Sci.*, *53*, 905–916.

Burkholder, J. B., J. J. Orlando, and C. J. Howard (1990), Ultraviolet absorption cross sections of Cl2O2 between 210 and 410 nm, *J. Phys. Chem.*, *94*, 687–695.

Canty, T., et al. (2005), Nighttime OClO in the winter Arctic vortex, *J. Geophys. Res.*, *110*, D01301, doi:10.1029/2004JD005035.

Chipperfield, M. P., A. M. Lee, and J. A. Pyle (1996a), Model calculations of ozone depletion in the Arctic polar vortex for 1991/92 to 1994/95, *Geophys. Res. Lett.*, *23*(5), 559–562.

Chipperfield, M. P., M. L. Santee, L. Froidevaux, G. L. Manney, W. G. Read, J. W. Waters, A. E. Roche, and J. M. Russell (1996b), Analysis of UARS data in the southern polar vortex in September using a chemical transport model, *J. Geophys. Res.*, *101*(D13), 18,861–18,881.

Danilin, M. Y., et al. (2003), Comparison of ER-2 aircraft and POAM-III, MLS, and SAGE-II satellite measurements during SOLVE using traditional correlative analysis and trajectory hunting technique, *J. Geophys. Res.*, *108*(D5), 8315, doi:10.1029/2001JD000781.

Davies, S., et al. (2003), Modeling the effect of denitrification on Arctic ozone depletion during winter 1999/2000, *J. Geophys. Res.*, *108*(D5), 8322, doi:10.1029/2001JD000445.

Deniel, C., J. P. Pommereau, R. M. Bevilacqua, and F. Lefèvre (1998), Arctic chemical depletion during the 1994–95 winter deduced from POAM II satellite observations and the REPROBUS 3-D model, *J. Geophys. Res.*, *103*(D15), 19,231–19,244.

De Zafra, R. L., M. Jaramillo, J. Barrett, L. K. Emmons, L. K. Emmons, P. M. Solomon, and A. Parrish (1989), New observations of a large concentration of ClO in the springtime lower stratosphere over Antarctica and its implications for ozone-depleting chemistry, *J. Geophys. Res.*, *94*(D9), 11,423–11,428.

Douglass, A. R., et al. (1997), A three-dimensional simulation of the evolution of the middle latitude winter ozone in the middle stratosphere, *J. Geophys. Res.*, *102*(D15), 19,217–19,232.

Goutail, F., et al. (1999), Total ozone depletion in the Arctic during the winters of 1993–94 and 1994–95, *J. Atmos. Chem.*, *32*, 1–34.

Hoppel, K. W., et al. (2003), POAM III observations of the anomalous 2002 Antarctic ozone hole, *Geophys. Res. Lett.*, *30*(7), 1394, doi:10.1029/2003GL016899.

Konopka, P., et al. (2004), Mixing and ozone loss in the 1999–2000 Arctic vortex: Simulations with the three-dimensional Chemical Lagrangian Model of the Stratosphere (ClaMS), *J. Geophys. Res.*, *109*, D02315, doi:10.1029/2003JD003792.

Konopka, P., et al. (2005), Mixing and chemical ozone loss during and after the Antarctic polar vortex major warming of September 2002, *J. Atmos. Sci.*, *62*, 848–859.

Lee, A. M., et al. (2000), Model and measurements show Antarctic ozone loss follows edge of polar night, *Geophys. Res. Lett.*, *27*(23), 3845–3848.

Lee, A. M., et al. (2001), The impact of the mixing properties within the Antarctic stratospheric vortex on ozone loss in spring, *J. Geophys. Res.*, *106*(D3), 3203–3211.

Lee, A. M., R. L. Jones, I. Kilbane-Dawe, and J. A. Pyle (2002), Diagnosing ozone loss in the extratropical lower stratosphere, *J. Geophys. Res.*, *107*(D11), 4110, doi:10.1029/2001JD000538.

Lefèvre, F., G. P. Brasseur, I. Folkins, A. K. Smith, and P. Simon (1994), Chemistry of the 1991–1992 stratospheric winter: Three-dimensional model simulations, *J. Geophys. Res.*, *99*(D4), 8183–8195.

Lucke, R. L., et al. (1999), The Polar Ozone and Aerosol Measurement (POAM) III instrument and early validation results, *J. Geophys. Res.*, *104*(D15), 18,785–18,799.

Lumpe, J. D., et al. (2002a), POAM III retrieval algorithm and error analysis, *J. Geophys. Res.*, *107*(D21), 4575, doi:10.1029/2002JD002137.

Lumpe, J. D., et al. (2002b), Comparison of POAM III ozone measurements with correlative aircraft and balloon data during SOLVE, *J. Geophys. Res.*, *108*(D5), 8316, doi:10.1029/2001JD000472.

MacKenzie, I. A., et al. (1996), Chemical loss of polar vortex ozone inferred from UARS MLS measurements of ClO during the Arctic and Antarctic late winters of 1993, *J. Geophys. Res.*, *101*(D9), 14,505–14,518.

Manney, G. L., et al. (2003), Lower stratospheric temperature differences between meteorological analyses in two cold Arctic winters and their impact on polar processing studies, *J. Geophys. Res.*, *108*(D5), 8328, doi:10.1029/2001JD001149.

Morris, G. A., et al. (2005), A review of the Match technique as applied to AASE-2/EASOE and SOLVE/THESEO 2000, *Atmos. Chem. Phys.*, *4*, 4665–4717.

Nash, E. R., et al. (1996), An objective determination of the polar vortex using Ertel's potential vorticity, *J. Geophys. Res.*, *101*(D5), 9471–9478.

Nedoluha, G. E., et al. (2003), POAM III measurements of PSCs and water vapor in the 2002 Antarctic vortex, *Geophys. Res. Lett.*, *30*(15), 1796, doi:10.1029/2003GL017577.

Newman, P. A., et al. (1998), Meteorological atlas of the Southern Hemisphere lower stratosphere for August and September 1987, *NASA Tech. Memo*, *TM-4049*, 131 pp.

Pfeilsticker, K., et al. (2000), Lower stratospheric organic and inorganic bromine budget for the arctic winter 1998/99, *Geophys. Res. Lett.*, *27*(20), 3305–3308.

Prados, A. I., et al. (2003), POAM III ozone in the upper troposphere and lowermost stratosphere: seasonal variability and comparisons to aircraft observations, *J. Geophys. Res.*, *108*(D7), 4218, doi:10.1029/2002JD002819.

Randall, C. E., et al. (2003), Validation of POAM III ozone: Comparisons with ozonesondes and satellite data, *J. Geophys. Res.*, *108*(D12), 4367, doi:10.1029/2002JD002944.

Rex, M., et al. (1998), In-situ measurements of stratospheric ozone depletion rates in the Arctic winter 1991/1992: A Lagrangian approach, *J. Geophys Res.*, *103*(D5), 5843–5853.

Rex, M., et al. (1999), Chemical ozone loss in the Arctic winter 1994/95 as determined by the Match technique, *J. Atmos. Chem.*, *32*(1), 35–59.

Rex, M., et al. (2002), Chemical loss of Arctic ozone in winter 1999/2000, *J. Geophys. Res.*, *107*(D20), 8276, doi:10.1029/2001JD000533.

Rex, M., et al. (2003), On the unexplained stratospheric ozone losses during cold Arctic Januaries, *Geophys. Res. Lett.*, *30*(1), 1008, doi:10.1029/2002GL016008.

Rolph, G. D., and R. R. Draxler (1990), Sensitivity of three-dimensional trajectories to the spatial and temporal densities of the wind field, *J. Appl. Meteorol.*, *29*, 1043–1054.

Rosenfield, J. E., P. A. Newman, and M. R. Schoeberl (1994), Computations of diabatic descent in the stratospheric polar vortex, *J. Geophys. Res.*, *99*(D8), 16,677–16,689.

Salawitch, R. J., et al. (1993), Chemical loss of ozone in the Arctic vortex in the winter of 1991–92, *Science*, *261*, 1146–1149.

Salawitch, R. J., et al. (2005), Sensitivity of ozone to bromine in the lower stratosphere, *Geophys. Res. Lett.*, *32*, L05811, doi:10.1029/2004GL021504.

Sander, S. P., et al. (2003), Chemical kinetics and photochemical data for use in atmospheric studies, evaluation number 14, *JPL Publ., 02-25*, Jet Propul. Lab., Pasadena, Calif.

Santee, M. L., G. L. Manney, J. W. Waters, and N. J. Livesey (2003), Variations and climatology of ClO in the polar lower stratosphere from UARS Microwave Limb Sounder measurements, *J. Geophys. Res.*, *108*(D15), 4454, doi:10.1029/2002JD003335.

Sasano, Y., et al. (2000), ILAS observations of chemical ozone loss in the Arctic vortex during early spring 1997, *Geophys. Res. Lett.*, *27*(2), 213–216.

Schoeberl, M. R., et al. (1996), Development of the Antarctic ozone hole, *J. Geophys. Res.*, *101*(D15), 20,909–20,924.

Shindell, D. T., and R. L. de Zafra (1997), Limits on heterogeneous processing in the Antarctic spring vortex from a comparison of measured and modeled chlorine, *J. Geophys. Res.*, *102*(D1), 1441–1449.

Sinnhuber, B.-M., et al. (2003), Total ozone during the unusual Antarctic winter of 2002, *Geophys. Res. Lett.*, *30*(11), 1580, doi:10.1029/2002GL016798.

Stimpfle, R. M., et al. (2004), First measurements of ClOOCl in the stratosphere: The coupling of ClOOCl and ClO in the Arctic polar vortex, *J. Geophys. Res.*, *109*, D03301, doi:10.1029/2003JD003811.

Swinbank, R., and A. O'Neill (1994), A stratospheric-tropospheric data assimilation system, *Mon. Weather Rev.*, *122*, 6702–6886.

Terao, Y., Y. Sasano, H. Nakajima, H. L. Tanaka, and T. Yasunari (2002), Stratospheric ozone loss in the 1996/1997 Arctic winter: Evaluation based on multiple trajectory analysis for double-sounded air parcels by ILAS, *J. Geophys. Res.*, *107*(D24), 8210, doi:10.1029/2001JD000615.

Von der Gathen, P., et al. (1995), Observational evidence for chemical ozone depletion over the Arctic in winter 1991–92, *Nature*, *375*, 131–134.

Wamsley, P. R., et al. (1998), Distribution of halon-1211 in the upper troposphere and lower stratosphere and the 1994 total bromine budget, *J. Geophys. Res.*, *103*(D1), 1513–1526.

World Meteorological Organization (2003), WMO scientific assessment of ozone depletion: 2002, *Global Ozone Res. Monit. Proj. Rep. 47*, Geneva, Switzerland.

Wu, J., and A. E. Dessler (2001), Comparison between measurements and models of Antarctic ozone loss, *J. Geophys. Res.*, *106*(D3), 3195–3201.

R. Bevilacqua and K. Hoppel, Naval Research Laboratory, Washington, DC 20375-5320, USA. (karl.hoppel@nrl.navy.mil)

T. Canty, R. Salawitch, and M. Santee, Jet Propulsion Laboratory, California Institute of Technology, Pasadena, CA 91109, USA.